Global properties of proton-hole strengths in mass 54 to 70 nuclei

G. Mairle and M. Seeger
Max-Planck-Institut für Kernphysik, 6900 Heidelberg, Germany

M. Ermer, P. Grabmayr, A. Mondry, and G. J. Wagner
Physikalisches Institut der Universität Tübingen, 7400 Tübingen, Germany
(Received 20 November 1992)

A vector-polarized deuteron beam of 52 MeV was used to excite proton hole states via the ^{66}Zn($\vec{d}$,^{3}He)^{65}Cu reaction. From the measured angular distributions of differential cross sections $\sigma(\Theta)$ and analyzing powers $iT_{11}(\Theta)$ we determined spins and parities of a number of individual low-lying levels in ^{65}Cu and the hole strength distribution for $E_x < 19$ MeV. Relative proton occupancies, single-particle energies, the shape of the Fermi surface and spreading widths for various orbitals are presented as a result of a combined analysis with proton stripping reactions on ^{66}Zn. A corresponding analysis of previous proton pickup and stripping experiments on ^{54,56,58}Fe, ^{58,60,62,64}Ni, ^{64}Zn, and ^{70}Ge shows systematic A-dependent features of these integral properties of the spectra.

PACS number(s): 25.45.Hi, 27.50.+e, 21.10.Pc

I. INTRODUCTION

Many experiments have shown that the (d,^{3}He) reaction preferentially excites proton hole states and that reasonable spectroscopic results can be obtained with deuteron energies around 50 MeV (see, e.g., Refs. [1–4]). The use of a vector-polarized beam impinging on $J = 0$ nuclei allows unambiguous spin and parity determinations of final states based on pronounced structures of the differential cross sections $\sigma(\Theta)$ specific for the transferred angular momentum ℓ and features typical for the transferred total angular momentum j of the vector analyzing powers $iT_{11}(\Theta)$.

According to the compilation in Nuclear Data Sheets [5] ^{65}Cu has been the subject of numerous investigations. Measurement and analysis of nuclear reactions have led to considerable knowledge on the level scheme. It is, therefore, very astonishing to see that the spins of only the lowest states are definitely known, and that most of them were determined only indirectly by a combination of results from different reactions. Besides an early ^{66}Zn(d,^{3}He) experiment [6], which was restricted to excitation energies $E_x < 2.6$ MeV, the knowledge on proton hole states of ^{65}Cu comes from the ^{66}Zn(t,α) reaction [7,8]. This type of pickup reaction, however, suffers generally from the angular momentum mismatch. This circumstance leads to angular distributions whose unpronounced structures are quite unspecific with respect to the transferred ℓ values, and produces problems in determining reasonable spectroscopic factors. In addition, the level scheme deduced from the ^{66}Zn(t,α) reaction [7] for excitation energies $E_x > 3$ MeV is not compatible with the results of extensive investigations on γ decay of ^{65}Cu, and obviously was not used for the compilation of *adopted* levels in Nuclear Data Sheets [5].

Prompted by very satisfactory results [9–11] with the ($\vec{d}$,^{3}He) reactions on ^{64}Ni, ^{64}Zn, and ^{60}Ni when making use of strip-detector telescopes we decided to perform a careful investigation of the proton hole states of ^{65}Cu. The use of a polarized beam in connection with this type of particle detection allows for an unproblematic direct spin determination of low-lying, isolated states. In the region with a level density too high compared to the experimental energy resolution, an evaluation of the spectra by means of a superposition of *measured* angular distributions of $\sigma(\Theta)$ and $iT_{11}(\Theta)$ yields an ℓ, j decomposition of the strength distribution of proton hole states. Additionally in combination with proton stripping results [12] on ^{66}Zn the lowest-energy moments of the proton strength distributions can be determined, which give information on the shape and energetic position of the Fermi surface, on single-particle energies, and spreading widths. Since comparable experimental results exist for the (d,^{3}He) reactions on ^{54,56,58}Fe, Ref. [13], on ^{58,60,62,64}Ni, Refs. [9,10,14,15], on ^{64}Zn, Ref. [9], and on ^{70}Ge, Ref. [16], and also for the respective proton stripping reactions, Refs. [12, 17–21], it suggests itself to study the systematics of integral properties of proton single-particle strengths. In view of the known difficulties in determining absolute spectroscopic factors, however, the results from individual proton pickup and stripping reactions have to be normalized carefully, before a detailed comparison of the various nuclei can be made. The procedure has been outlined elsewhere [9, 11, 22, 23]. It will be reviewed in short and applied to ^{66}Zn in Sec. IV A. A compilation of the data for Fe, Ni, Zn, and Ge isotopes will be given in Secs. IV B–IV E.

II. EXPERIMENTAL PROCEDURE

The ^{66}Zn($\vec{d}$,^{3}He)^{65}Cu reaction was investigated with vector-polarized deuterons produced by an atomic beam source and accelerated to a kinetic energy of 52 MeV by the Karlsruhe isochronous cyclotron. A current of typically 15 nA was obtained on the target when the en-

ergy spread of the momentum-analyzing system was set to $\approx$ 70 keV. During the measurements a polarimeter [24] monitored the beam polarization, which was $P_y = 0.50 \pm 0.03$. The direction of polarization was flipped automatically after accumulation of a preset charge in the Faraday cup, typically every 20 sec. A 2 mg/cm^2 thick self-supporting zinc foil, isotopically enriched to 99% in ^{66}Zn, was used as a target. The reaction products were detected on one side of the beam with one Si-detector telescope consisting of a 250 μm thick ΔE strip detector and a large area surface barrier E detector (1500 μm). The ΔE counter was segmented in 10 strips of 2 mm width and 20 mm height, corresponding to an angular acceptance of 0.4 deg and a solid angle of 0.37 msr per strip. The efficiency of the strip detector has been checked before measurement with an α source and during the experiment by measuring cross sections at overlapping angles. The error of the absolute cross sections is estimated to 20%.

Angular distributions were measured between laboratory angles of 16° and 28°. The experience from the $(\vec{d},^3\mathrm{He})$ reactions on ^{64}Ni and ^{64}Zn obtained with the same experimental conditions [9] showed that it is this angular region of the analyzing powers which is characterized by opposite signs for spin-orbit partners of $\ell = 1$, $\ell = 2$, and $\ell = 3$ transitions. Even the analyzing power for $\ell = 0$ transfer exhibits a characteristic pattern at these angles. Hence the transferred angular momenta ℓ and j and consequently spins and parities of final states could be unambiguously determined from that part of the angular distributions of differential cross sections and analyzing powers. Experience from [8] also justifies the extraction of spectroscopic factors from differential cross sections measured in the narrow angular interval chosen. In the previous experiment a range of lab angles from 12° to 38° was covered which includes the first maxima of $1f_{5/2}$ and $1f_{7/2}$ angular distributions. The good distorted-wave Born approximation (DWBA) fits obtained over the full angular range suggest that reliable (relative) spectroscopic factors may also be obtained from data taken in the narrower angular range. The discussion of sum rule values below (Sec. IV A) will confirm this assumption.

Particle identification was achieved by conventional ΔE-E techniques. Details of the experimental techniques have been reported elsewhere [9, 25]. The overall energy resolution amounted to 110 keV mainly determined by the energy spread of the beam and the target thickness.

III. SPECTROSCOPIC RESULTS

Figure 1 shows a typical energy spectrum of ^{3}He particles measured at $\Theta_{\mathrm{lab}} = 22°$. In the region $0 \leq E_x \leq 5$ MeV we observe individual, strongly excited groups. The remaining part of the spectrum, extending to excitation energies of 19 MeV, exhibits a rather structureless continuum. The background given as a smooth curve in Fig. 1 represents the result of a careful analysis of all the spectra (see below). Isolated groups for $E_x < 4$ MeV are not affected. The limited energy resolution of 110 keV only

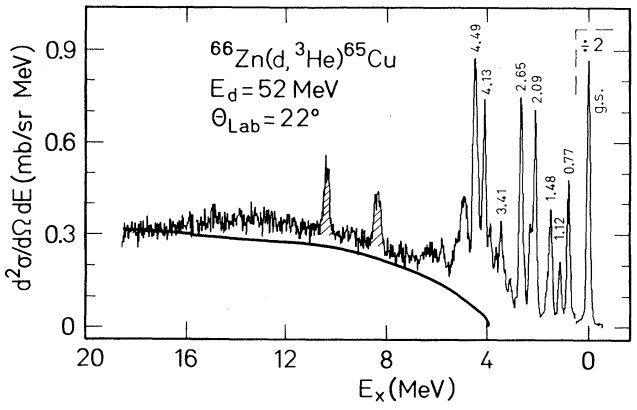

FIG. 1. Spectrum of the ^{66}Zn$(d,^3$He$)^{65}$Cu reaction. The smooth line characterizes the background as determined from an analysis of all spectra.

allows a direct evaluation of isolated levels at 0, 0.771, 1.116, 2.094, and 2.278 MeV. Between 2.4 MeV and 6 MeV the spectra were analyzed by setting windows of appropriate width on the observed structures, and, for excitation energies above 6 MeV, by evaluating energy bins of 1 MeV widths.

Figures 2, 3, 4, and 5 show the resulting angular distributions of differential cross sections $\sigma(\Theta)$ and analyzing powers $iT_{11}(\Theta)$ compared to DWBA calculations. The optical model parameters which are given in Table I are the results of an analysis of elastically scattered polarized deuterons [25] measured at 52 MeV, and of elastically scattered ^{3}He particles [26] measured at 37.7 MeV. Generally a satisfactory fit to the data of Figs. 2, 3, and 4 could be obtained. As the measured angular distributions of $\sigma(\Theta)$ and $iT_{11}(\Theta)$ are characteristic for the ℓ and j values of the transferred proton, and as their structures are quite insensitive [3] against changes of the Q value, the determination of spin and parity of final states in ^{65}Cu is mainly based on a comparison with *measured* angular distributions of transitions leading to final states with known spin in neighboring nuclei. The comparison with DWBA calculations serves as an additional check and also provides the desired spectroscopic factors. This method has been successfully applied to nuclei in different mass regions [9, 11, 22, 23, 26, 28].

Inspection of the measured angular distributions in Figs. 2–5 immediately shows that the quality of a measurement with a strip detector is superior to one performed with independent detectors, because normalization problems disappear and the scatter of the data points is mainly of statistical nature. This offers the possibility to decompose unresolved groups or energy bins using measured angular distributions of isolated and strongly excited levels with known spins, and the results are clearly superior to those from a superposition of DWBA curves. Unresolved groups containing up to three components with different j transfer can be decomposed under favorable conditions, i.e., if the statistical accuracy of the spectra is sufficient and the constituents are excited with comparable intensity. This has been exem-

plified in detail in Ref. [11]. In the following we give a detailed discussion of our results and compare them, wherever possible, with the adopted level scheme of the Nuclear Data Sheets [5].

The ground state of ^{65}Cu: Spin and parity $j^\pi = \frac{3}{2}^-$ have been assigned on the basis of the $L = 0$ transfer observed in the ^{63}Cu$(t,p)^{65}$Cu(g.s.) reaction [29]. This is confirmed by the angular distribution of differential cross section ($\ell = 1$) and analyzing power ($j = \frac{3}{2}$) given in Fig. 2.

$E_x = 0.771$ MeV: $J^\pi = \frac{1}{2}^-$ has been assigned on the basis of combined results of γ work [5] giving $J = \frac{1}{2}$, and proton stripping reactions [5, 20] giving $J^\pi = \frac{1}{2}^-, \frac{3}{2}^-$. The result is confirmed by our direct spin determination, see Fig. 2.

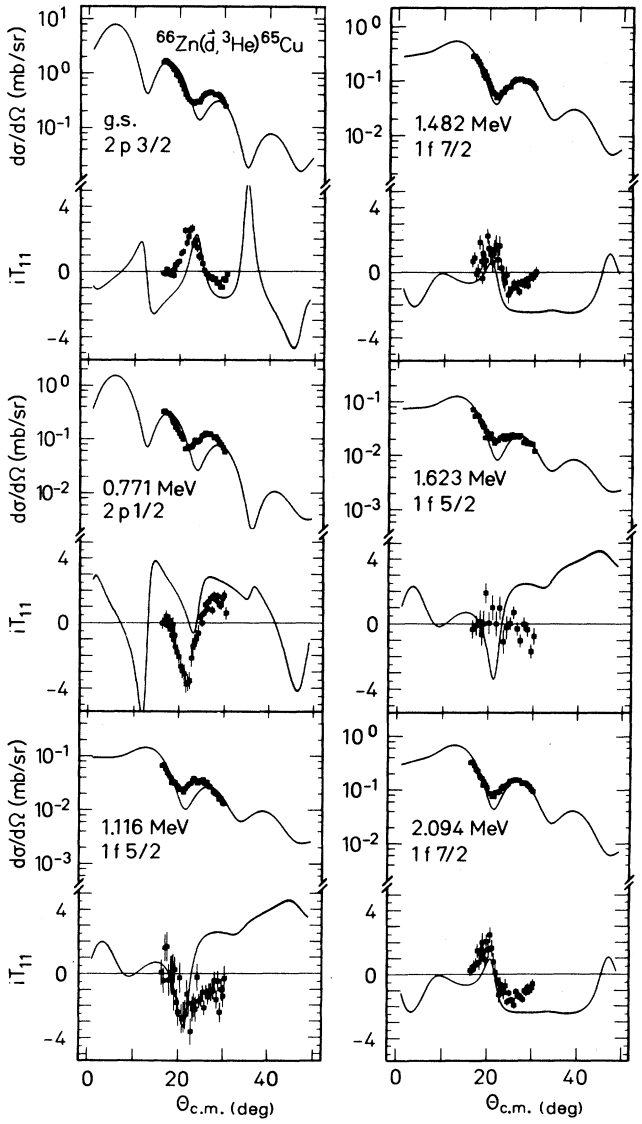

FIG. 2. Angular distributions of differential cross sections and analyzing powers from the ^{66}Zn$(\vec{d},^3$He$)^{65}$Cu reaction for individual levels and for energy bins compared to DWBA calculations.

$E_x = 1.116$ MeV: $J^\pi = \frac{5}{2}^-$ has been deduced from the combined results of (γ,γ'), β decay, Coulomb excitation, and proton stripping on ^{64}Ni, Ref. [5], in agreement with our result.

$E_x = 1.482$ MeV: The combined results from the ^{64}Ni(^{3}He,d) reaction, allowed β decay of ^{65}Ni, Coulomb excitation, and inelastic scattering [5] yield $J^\pi = \frac{7}{2}^-$, which agrees with $1f_{7/2}$ proton pickup as observed in the present experiment.

$E_x = 1.623$ MeV: In spite of weak excitation and incomplete separation from the neighboring $\frac{7}{2}^-$ state at 1.482 MeV, the measured angular distributions are in fa-

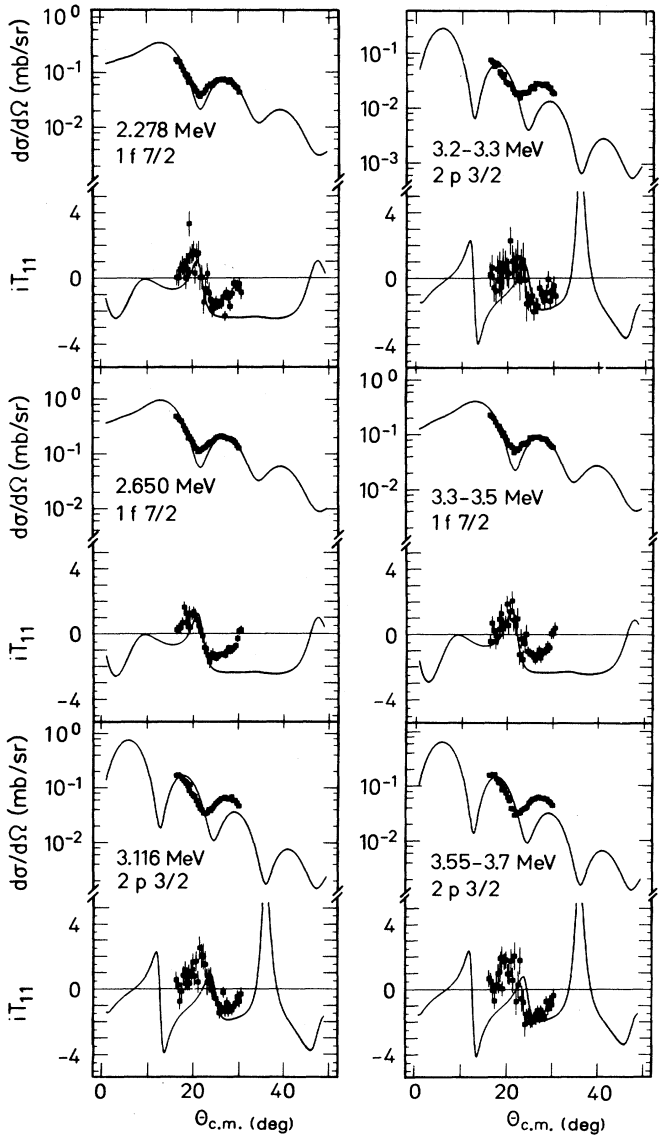

FIG. 3. Angular distributions of differential cross sections and analyzing powers from the ^{66}Zn$(\vec{d},^3$He$)^{65}$Cu reaction for individual levels and for energy bins compared to DWBA calculations. For the energy intervals [3.20,3.30] only the residual angular distributions following subtraction of a pure $f_{7/2}$ distribution (with a spectroscopic factor as given in Table II) are shown.

TABLE I. Optical model parameters used in DWBA calculations.

	V (MeV)	r_v (fm)	a_v (fm)	W (MeV)	r_w (fm)	a_w (fm)	r_c (fm)	$V_{s.o.}$ (fm)	$r_{s.o.}$ (fm)	$a_{s.o.}$
d[a]	79.8	1.15	0.802	9.57	1.68	0.785	1.30	6.68	1.11	0.452
^{3}He[b]	168.66	1.147	0.707	28.18	1.507	0.793	1.30			
p	[c]	1.20	0.65				1.30	$\lambda = 25$		

[a] Reference [26].
[b] Reference [27].
[c] Adjusted to reproduce the experimental binding energy.

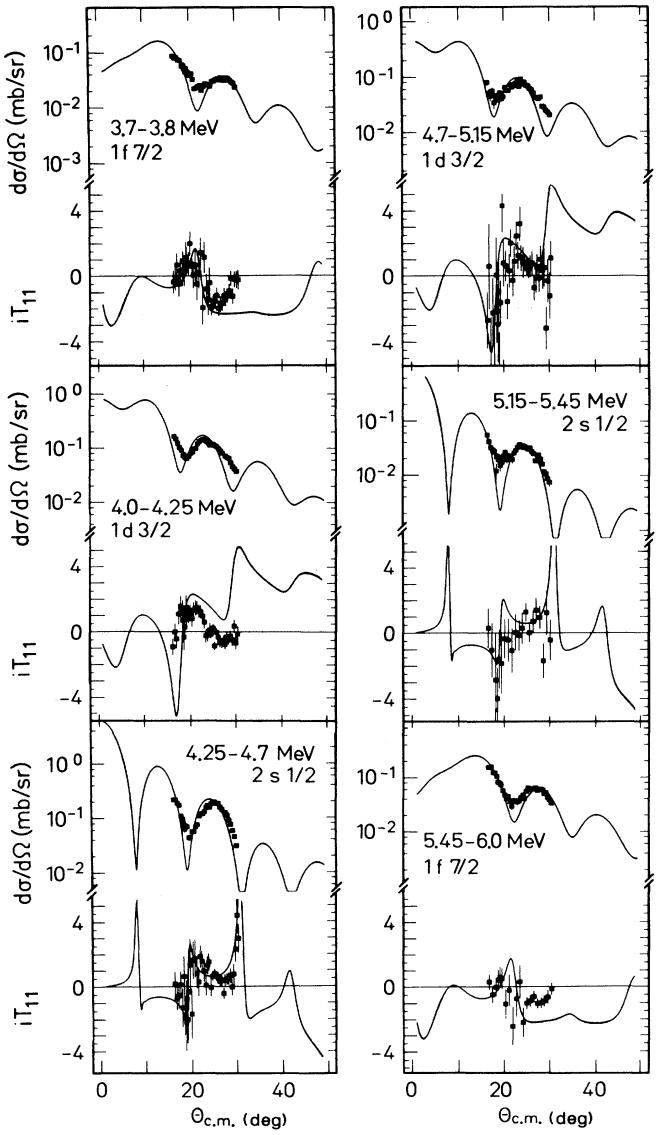

FIG. 4. Angular distributions of differential cross sections and analyzing powers from the ^{66}Zn($\vec{d}$,^{3}He)^{65}Cu reaction for various energy bins compared to DWBA calculations. For the energy intervals [4.25,4.70] and [5.15,5.45] only the residual angular distributions following subtraction of a pure $f_{7/2}$ distribution (with a spectroscopic factor as given in Table II) are shown.

vor of $1f_{5/2}$ transfer and are, therefore, compatible with spin and parity $J^\pi = \frac{5}{2}^-$, which is the combined result from different sources [5].

E_x = 2.094 MeV: We uniquely determine spin and parity $J^\pi = \frac{7}{2}^-$, which confirms the tentative values $J^\pi = (\frac{7}{2})^-$ of Ref. [5] resulting from (p,γ), inelastic scattering and (t,α) experiments.

E_x = 2.278 MeV: In the present experiment this level is not resolved from the $(\frac{1}{2}^-)$ state at 2.213 MeV which, however, was observed to be extremely weakly excited in the ^{66}Zn(t,α) reaction [7]. The measured $\ell = 3, j = 7/2$ angular distributions of Fig. 3 lead, therefore, to spin and parity $J^\pi = \frac{7}{2}^-$, compatible with $J^\pi = (\frac{7}{2}^-)$ as suggested in Ref. [5].

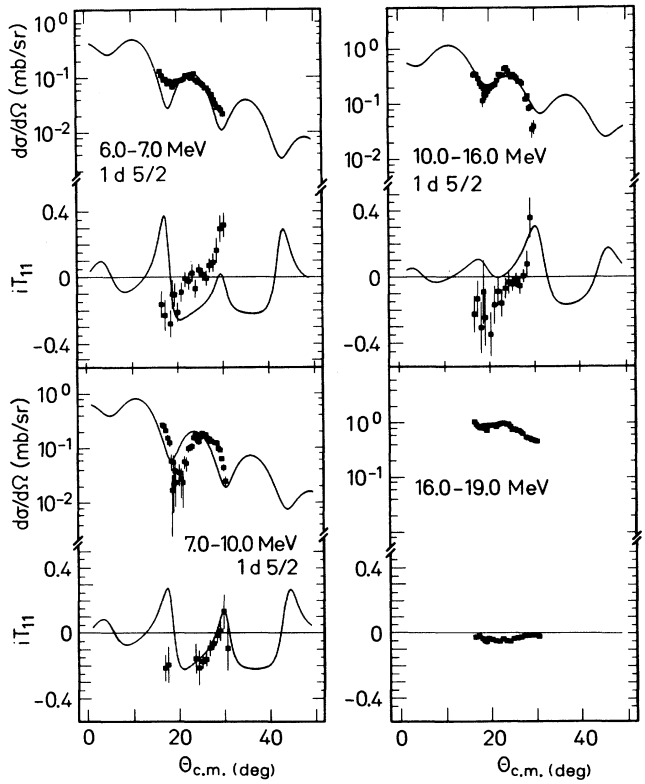

FIG. 5. Angular distributions of differential cross sections and analyzing powers from the ^{66}Zn($\vec{d}$,^{3}He)^{65}Cu reaction in the continuum region between 6 MeV and 19 MeV excitation energy.

E_x = 2.650 MeV: The present data give unambiguously $J^\pi = \frac{7}{2}^-$, because the energetically unresolved states at 2.593 MeV, $J^\pi = (\frac{1}{2}^-, \frac{5}{2}^-)$ and at 2.753 MeV, $J^\pi = (\frac{7}{2}^+, \frac{5}{2}^+)$ are known to be comparatively weakly excited in pickup reactions [7, 8]. The result is in agreement with observed $\ell = 3$ transfer seen in stripping [20] and pickup [7] reactions.

E_x = 3.116 MeV: This level was excited via $\ell = 1$ transfer in stripping [20] giving $J^\pi = (\frac{1}{2}^-, \frac{3}{2}^-)$ in Ref. [5]. The present experiment allows a unique $J^\pi = \frac{3}{2}^-$ assignment.

TABLE II. Summary of the ^{66}Zn($\vec{d}$,^{3}He)^{65}Cu results.

E_x (keV)[a]	E_x (keV)[b]	ΔE_x (MeV)[c]	J^π [d]	J^π [e]	C^2S [f]
g.s.	0		$\frac{3}{2}^-$	$\frac{3}{2}^-$	0.90
770.66(9)	774		$\frac{1}{2}^-$	$\frac{1}{2}^-$	0.21
1115.556(4)	1119		$\frac{5}{2}^-$	$\frac{5}{2}^-$	0.30
1481.83(3)	1507	1.25 – 1.80	$\frac{7}{2}^-$	$\frac{7}{2}^-$	0.67
1623.43(5)			$\frac{5}{2}^-$	$(\mathbf{\frac{5}{2}}, \frac{7}{2})^-$	0.28
1725.00(5)			$\frac{3}{2}^-$		
2094.32(14)	2080		$(\frac{7}{2})^-$	$\frac{7}{2}^-$	0.91
2278.4(9)	2288		$(\frac{7}{2})^-$	$\frac{7}{2}^-$	0.48
2649.67(13)	2645	2.40 – 2.90	$(\frac{5}{2}^-, \frac{7}{2}^-)$	$\frac{7}{2}^-$	1.41
3116(3)	3096	2.90 – 3.20	$(\frac{1}{2}^-, \frac{3}{2}^-)$	$\frac{3}{2}^-$	0.13
	3252	3.20 – 3.30	$(\frac{3}{2}^+, \frac{5}{2}^+)$[g]	$\frac{3}{2}^-$	0.05
				$+\frac{7}{2}^-$	0.21
	3408	3.30 – 3.50		$\frac{7}{2}^-$	0.69
	3623	3.55 – 3.70		$(\mathbf{\frac{3}{2}}^-, \frac{7}{2}^-)$	0.11,0.51
	3748	3.70 – 3.80		$\frac{7}{2}^-$	0.29
	3901	3.80 – 4.00		$(\frac{5}{2}, \mathbf{\frac{7}{2}})^-$	(0.67,0.34)
	4125	4.00 – 4.25		$\frac{3}{2}^+$	1.38
	4487	4.25 – 4.70		$\frac{7}{2}^-$	0.50
				$\frac{1}{2}^+$	0.55
				$\frac{7}{2}^-$	0.51
	4928	4.70 – 5.15		$\frac{3}{2}^+$	0.88
				$+\frac{7}{2}^-$	0.80
	5292	5.15 – 5.45		$(\frac{5}{2}, \mathbf{\frac{7}{2}})^-$	(0.56,0.29)
				$+\frac{1}{2}^+$	0.10
	5732	5.45 – 6.00		$\frac{7}{2}^-$	0.64
	6486	6.00 – 7.00		$(\mathbf{\frac{3}{2}}, \frac{5}{2})^+$	(1.58,0.88)
				$+\frac{7}{2}^-$	0.32
	7505	7.00 – 8.00		$(\frac{3}{2}, \frac{5}{2})^+$	(1.27,0.71)
	8535	8.00 – 9.00		$\frac{5}{2}^+$	0.90
	9483	9.00 – 10.00		$\frac{5}{2}^+$	0.48
	10513	10.00 – 11.00		$\frac{5}{2}^+$	1.17
	11502	11.00 – 12.00		$\frac{5}{2}^+$	0.90
	12503	12.00 – 13.00		$\frac{5}{2}^+$	1.75
	13501	13.00 – 14.00		$\frac{5}{2}^+$	1.75
	14501	14.00 – 15.00		$\frac{5}{2}^+$	1.58
	15498	15.00 – 16.00		$\frac{5}{2}^+$	1.09

[a] Excitation energies from Ref. [5].

[b] Present experiment: Deduced excitation energies for resolved states and centroid energy bins with unresolved states.

[c] Excitation energy range of the investigated energy bins.

[d] Spins and parities from Ref. [5].

[e] Present experiment: Deduced spins and parities. For ambiguous assignments preferred values are given in bold face.

[f] Present experiment: Renormalized spectroscopic factors (original $C^2S \times 0.70$, see Sec. IV A).

[g] Reference [7].

Above $E_x = 3.2$ MeV the situation is rather confusing. Excitation energies from the high resolution ^{66}Zn(t,α) reaction [7] could not be related [5] to those obtained from γ decay. The present contribution improves the situation to the extent that we determine spins and parities of the spectroscopic pickup strengths prevailing in narrow energy bins.

The method of decomposing unresolved groups with respect to their l,j contributions, which was mentioned above, has been applied. To be exact, the decomposition of angular distributions was performed simultaneously for differential cross sections obtained with deuteron "spin up" as well as "spin down" in order to exploit the j-transfer information. Angular distributions of differential cross sections and analyzing powers calculated from the remaining (spin-up and spin-down) cross sections are given in Figs. 3 and 4. The corresponding DWBA calculations have been performed with the correct binding energies and the resulting spectroscopic factors are given in Table II.

The energy bin [3.20,3.30] MeV contains $2p_{3/2}$ and $1f_{7/2}$ strength. The following bins [3.30,3.50] MeV, [3.55,3.70] MeV, and [3.70,3.80] MeV are excited predominantly by $1f_{7/2}$, $2p_{3/2}$, and $1f_{7/2}$ pickup, respectively. A narrow peak at 4.125 MeV represents a large fraction of the $1d_{3/2}$ proton hole strength. For excitation energies above $E_x = 4$ MeV a background of ^{3}He particles was subtracted, whose angular distributions were determined in the high-energy part of the spectra between 16 and 19 MeV, see Fig. 5. It turned out that the "background" defined by this angular distribution increases monotonically with excitation energy. An interpolation (spline) of the values obtained for the different energy bins given in Table II is shown in the spectrum of Fig. 1. The remaining part of the cross section shows well-structured angular distributions up to 16 MeV of excitation; compare Figs. 3–5.

A careful decomposition of the prominent group contained in the energy interval [4.25,4.70] MeV shows the excitation of a triplet of states with the spin sequence $\frac{7}{2}^-, \frac{1}{2}^+, \frac{7}{2}^-$. The energy region [4.70,7.00] MeV, which is characterized by unresolved broad structures in the spectrum of Fig. 1, obviously represents the transition region between pickup from the $1f_{7/2}$ and $(2s,1d)$ shells (Table II). The region between 7 and 16 MeV appears as a structureless continuum of states, predominantly excited by pickup from the $1d_{5/2}$ shell (Fig. 5).

IV. MOMENTS OF THE PROTON STRENGTH DISTRIBUTIONS

A. Normalization of pickup and stripping reaction data

We have seen in Sec. III that we can assign spins and parities to low-lying levels and determine their spectroscopic strengths by means of the $(\vec{d},^3\mathrm{He})$ reaction, and that we can deduce integral properties of the spectra in the region of high level density. From these data we calculate the lowest-energy moments of the different (nlj) strength distributions. Spectroscopic factors were obtained with standard nonlocal zero-range DWBA calculations applying the separation energy method and with commonly used bound state parameters (see Table I). Since the spectroscopic factors are known to depend sensitively on these parameters, they were normalized according to a method outlined in Ref. [22]. In short, for a complete set of spectroscopic data obtained from stripping (+) and pickup (−) reactions on a given target nucleus, the shell model requires

$$(G^+_{nlj} + G^-_{nlj})/(2j+1) = 1$$

for a subshell with quantum numbers (nlj). Assuming that (i) the *relative* values for various (nlj) values of the summed stripping strengths G^+_{nlj} and pickup strengths G^-_{nlj} within each experiment can be determined correctly by means of a DWBA analysis, and that (ii) the complete strengths were observed, we have to adjust only two normalization factors f^+ and f^- to ensure that the relation given above holds simultaneously for all shells involved. A critical evaluation of such a procedure is given in Ref. [11]. Application to the present ^{66}Zn$(\vec{d},^3$He) data and the ^{66}Zn(^{3}He,d) data of Ref. [12] yields normalization factors $f^- = 0.70$ and $f^+ = 1.02$ which have been determined by linear regression. Only the $1f_{7/2}, 2p_{3/2}, 2p_{1/2}$, and $1f_{5/2}$ subshells, which have been observed in both the stripping and the pickup reactions, were included in the fit. The renormalized spectroscopic factors of the present pickup experiment are given in Table II together with the other spectroscopic results. The summed spectroscopic strengths G^+_{nlj} and pickup strengths G^-_{nlj} are given in Table III. From these values we can judge the quality of the data and of the normalization procedure. The total renormalized $(1f,2p)$ pickup strength $\sum_{nlj} G^-_{nlj} = 10.03$, and the total $(1f,2p)$ stripping strength $\sum_{nlj} G^+_{nlj} = 10.34$ are close to the shell model expectation values of 10, which is the number of protons as well as the number of proton holes in the $(1f,2p)$ shell of ^{66}Zn. The individual summed strengths $(G^+_{nlj} + G^-_{nlj})$ show an average deviation of 10% from $(2j+1)$. For the pickup strengths from the $(2s,1d)$ shell, which have not been included in the fit, we observe larger deviations from the shell model expectation values. Possible reasons for missing the $2s_{1/2}$ strength have been discussed in Ref. [11]. The excessive $1d$ strengths are the result of the uncertainty of the evaluation of the continuum; an insignificantly increased background between 6 MeV and 16 MeV would reduce them to allowed values.

Similarly, we treated pickup and stripping data (updated, if necessary) on ^{54,56,58}Fe, Refs. [13, 17–19], on ^{58,60,62,64}Ni, Refs. [9, 10, 14, 15, 20], on ^{64}Zn, Refs. [9, 12], and on ^{70}Ge, Refs. [16, 21] to obtain a compilation of the lowest-energy moments of the proton strength distributions in nuclei around the $1f_{7/2}$ proton shell closure. These are occupation numbers, single-particle energies, and spreading widths, respectively.

TABLE III. Integral properties of proton spectra measured in stripping (+) and pickup (−) reactions on ^{66}Zn. The four $(1f, 2p)$ subshells were used for the normalization of the spectroscopic strengths $G^{\pm}_{nlj}$. Energy centroids $\langle E^{\pm}_{nlj}\rangle$, single-particle energies E_{nlj}, and widths $\sqrt{M_2^-(nlj)}$ are given in MeV.

nlj	G^+_{nlj}	G^-_{nlj}	$\frac{G^+_{nlj}+G^-_{nlj}}{2j+1}$	$\langle E^+_{nlj}\rangle$	$\langle E^-_{nlj}\rangle$	E_{nlj}	$\sqrt{M_2^-(nlj)}$
$1f_{5/2}$	6.25	0.58	1.14	0.68	1.36	−5.07	0.25
$2p_{1/2}$	1.64	0.23	0.94	0.88	0.77	−5.04	0.00
$2p_{3/2}$	2.12	1.19	0.83	0.51	0.78	−6.54	1.43
$1f_{7/2}$	0.33	8.03	1.04	1.21	3.59	−12.19	1.41
$1d_{3/2}$	0.00	5.12	1.28		5.84	−14.76	1.33
$2s_{1/2}$	0.00	0.65	0.33		4.61	−13.54	0.29
$1d_{5/2}$	0.00	9.61	1.60		12.49	−21.42	2.09

B. Proton occupancies

The lowest (zeroth) moments of the proton strength distributions are the summed stripping strengths (for $J = 0$ target nuclei) $G^+_{nlj} = \sum_i (2j+1) C^2 S^{(i)}_{nlj}$ and pickup strengths $G^-_{nlj} = \sum_i C^2 S^{(i)}_{nlj}$, which define the number of proton holes $\bar{p}_{nlj}$ and proton particles p_{nlj}, respectively, in a shell with quantum numbers nlj. The requirement that $\bar{p}_{nlj} + p_{nlj} = 2j + 1$ in the average has been used for the normalization procedure. As both quantities G^-_{nlj} and $(2j+1-G^+_{nlj})$ independently determine the number p_{nlj} of protons in the orbit with quantum numbers nlj, we calculated the proton occupation probability v^2_{nlj} according to their mean value

$$v^2_{nlj} = (G^-_{nlj} + 2j + 1 - G^+_{nlj})/2(2j+1) \ .$$

In those cases, where G^-_{nlj} or G^+_{nlj} (slightly) exceeded the shell model expectation values, they were set equal to $(2j+1)$. A compilation of the resulting values of v^2_{nlj} in the $(2s, 1d)$ and the $(1f, 2p)$ shells of iron, nickel, zinc, and germanium isotopes is given in Table IV.

TABLE IV. Integral properties of proton spectra. For each of the nuclei the first line gives the single-particle energy $-E_{nlj}$ in MeV as defined in Sec. IV C, the second line gives the proton occupation probability v^2_{nlj} (see Sec. IV B), and the third line gives the widths $\sqrt{M_2^-(nlj)}$ in MeV (see Sec. IV E) of the proton hole strength distributions.

	$1d_{5/2}$	$2s_{1/2}$	$1d_{3/2}$	$1f_{7/2}$	$2p_{3/2}$	$2p_{1/2}$	$1f_{5/2}$
^{54}Fe		11.8	12.9	7.9	2.4	0.9	1.3
		0.88	0.95	0.64	0.09	0.05	0.01
		0.7	1.3	1.5	0.5	0.0	1.4
^{56}Fe		12.9	13.3	9.3	4.9	3.2	2.9
		0.87	1.00	0.71	0.14	0.27	0.16
		1.0	0.7	1.0	1.2	0.0	1.1
^{58}Fe		14.9	14.6	10.8	6.5		
		0.86	1.00	0.64	0.06		
		1.5	0.8	1.2	0.0		
^{58}Ni	16.3	11.2	12.1	8.1	2.9	1.4	1.6
	1.00	0.99	1.00	0.91	0.04	0.03	0.06
	1.7	0.00	0.6	1.0	0.7	0.0	0.5
^{60}Ni	20.2	12.2	13.6	10.1	5.0	3.3	3.2
	1.00	0.83	0.99	0.90	0.10	0.01	0.05
	3.1	0.0	1.1	1.7	0.8	0.0	0.0
^{62}Ni		13.6	14.7	11.1	7.3	4.7	4.3
		1.00	1.00	0.90	0.21	0.00	0.00
		0.6	1.0	1.3	0.4	0.0	0.0
^{64}Ni	22.7	14.7	17.0	13.3	7.9	6.3	5.6
	1.00	0.74	0.97	0.97	0.16	0.01	0.00
	2.1	0.0	1.3	1.4	0.3	0.0	0.0
^{64}Zn	21.2	12.1	15.4	10.9	5.8	4.5	3.8
	1.00	0.81	1.00	1.00	0.46	0.31	0.11
	2.0	0.3	1.5	1.4	1.5	0.0	0.4
^{66}Zn	21.4	13.5	14.8	12.2	6.5	5.0	5.1
	1.00	0.66	1.00	0.98	0.42	0.14	0.05
	2.1	0.3	1.3	1.4	1.4	0.0	0.3
^{70}Ge		13.5		12.1	7.4		5.5
		0.65		1.00	0.61		0.23
		0.7		1.5	1.1		0.4

C. Proton single-particle energies

From the proton strength distributions measured in stripping and pickup reactions we deduce single-particle energies according to the widely accepted definition:

$$E_{nlj}(A) = [G^+_{nlj} E^+_{nlj}(A) + G^-_{nlj} E^-_{nlj}(A)]/(G^+_{nlj} + G^-_{nlj}) \ .$$

This equation defines single-particle energies $E_{nlj}(A)$ as the energy centroid for stripping and pickup reactions on a target nucleus A and a given shell (nlj) weighted with the respective stripping (G^+_{nlj}) and pickup (G^-_{nlj}) strengths. The energies E^+_{nlj} and E^-_{nlj} are obtained from the first energy moments of the strength distributions, i.e., the centroids of the excitation energies $\langle E^+_{nlj}\rangle$ and $\langle E^-_{nlj}\rangle$ in the final nuclei $(A+1)$ and $(A-1)$, respectively, and the proton ground state separation energies B according to

$$E^+_{nlj}(A) = -B(A+1) + \langle E^+_{nlj}\rangle$$

and

$$E^-_{nlj}(A) = -B(A) - \langle E^-_{nlj}\rangle \ .$$

In the case of ^{66}Zn, which is the subject of the present pickup experiment, the quantities $\langle E^+_{nlj}\rangle$, $\langle E^-_{nlj}\rangle$, and the resulting values of the single-particle energies E_{nlj} are

given separately in Table III. A compilation of single-particle energies of all 10 nuclei considered is shown in Table IV.

Generally, proton single-particle energies increase monotonically with increasing neutron number N and they decrease monotonically with increasing proton number Z. In certain regions of the mass table, which are limited by shell closures, the single-particle energies exhibit a *linear* dependence on N and Z. This could be shown, e.g., in Refs. [9, 22, 23, 30]. The 10 nuclei of the present investigation are situated around the $1f_{7/2}$ proton shell closure. The linear functions

$$E_{nlj}(N,Z) = E_{nlj}(^{56}\mathrm{Ni}) + a_{nlj}N + b_{nlj}Z$$

show in general different slopes for nuclei below or above ^{56}Ni. This is the reason why we renounce a parametrization in the spirit of Ref. [30]. For studies in neighboring mass regions, the knowledge of single-particle energies in nuclei in the direct vicinity of ^{56}Ni is, however, useful because $E_{nlj}(^{56}\mathrm{Ni})$ is not directly accessible (except for transfer reactions with radioactive beams and inverse kinematics), but might be determined through linear extrapolation with the above equation. Due to extreme mixing in the $(1f, 2p)$ shell an extraction of effective particle-hole interactions according to the ideas of Bansal and French [31] is also not indicated.

D. The Fermi surface for protons

The combination of measured proton occupation numbers and corresponding single-particle energies offers the possibility to probe the shape of the Fermi surface. This representation shows very intuitively the degree of core excitations. A fit with the commonly used BCS function defines position and shape of the Fermi surface. A parametrization according to

$$v^2_{nlj} = \frac{1}{2}\left\{1 - (E_{nlj} - E_F)/\sqrt{(E_{nlj} - E_F)^2 + \Delta^2}\right\}$$

allows one to determine the Fermi energy E_F and the "gap parameter" Δ, a measure of the extent of particle-hole excitations. In Fig. 6 we show the results obtained for ^{66}Zn, when we use both the pickup and the stripping data from Table III for the calculation of v^2_{nlj} as obtained in Sec. IV B. Squares indicate data for the $(1f, 2p)$ shells, which were included in the fit, circles stand for the $(2s, 1d)$ shell not included. Table V contains the parameters E_F and Δ which have been consistently calculated[1] for all investigated nuclei with proton occupation probabilities as defined in Sec. IV B.

[1]We take the opportunity to call the reader's attention to values of E_F and Δ for even Ni isotopes given in Table 4 of Ref. [11], which have been erroneously calculated only on the basis of pickup data.

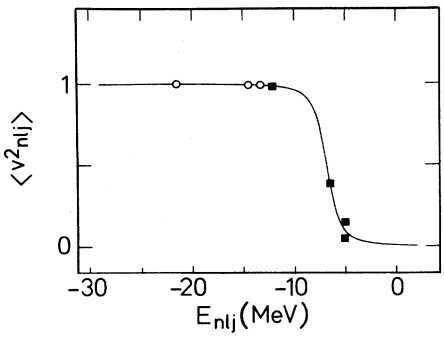

FIG. 6. Fermi surface for protons in ^{66}Zn: proton occupation probability v^2_{nlj} vs single-particle energies E_{nlj} with the shell sequence $1d_{5/2}, 1d_{3/2}, 2s_{1/2}, 1f_{7/2}, 2p_{3/2}, 1f_{5/2}$, and $2p_{1/2}$ corresponding to decreasing v^2_{nlj}. We show the result of a fit with a BCS function to both pickup and stripping data from the $(1f, 2p)$ shells (squares). The $(2s, 1d)$ shells were not included in the fit; circles mark their single-particle energies.

E. Spreading widths

The extent to which single hole states are split due to residual interactions can be quantified by the second energy moments $M_2^-(nlj)$ of the strength distributions measured in pickup reactions. They can be calculated according to the relation

$$M_2^-(nlj) = \sum_i (E_i^- - \langle E^-_{nlj}\rangle)^2 C^2S_i^- \Big/ \sum_i C^2S_i^-$$

from the respective excitation energies E_i^- of individual final states and their energy centroids $\langle E^-_{nlj}\rangle$. For Gaussian distributions the second moments are related to the spreading widths according to $\Gamma^{\downarrow} = 2.35\sqrt{M_2^-}$. The compilation in Table IV contains the values $\sqrt{M_2^-(nlj)}$. Because they depend sensitively on the high-energy tails of the hole strength distributions, rather large absolute errors may be expected, whose size we feel unable to estimate. Relative changes in chains of isotopes, however, should be more precisely defined, because smoothly varying strength distributions may be assumed, and because

TABLE V. Parameters of the Fermi surface for protons. We use the BCS function for the proton occupation probability $v^2_{nlj} = \frac{1}{2}\left[1 - (E_{nlj} - E_F)/\sqrt{(E_{nlj} - E_F)^2 + \Delta^2}\right]$.

	$-E_F$ (MeV)	Δ (MeV)
^{54}Fe	7.1 ± 0.3	2.8 ± 0.6
^{56}Fe	7.9 ± 0.2	2.8 ± 0.3
^{58}Fe	10.2 ± 0.1	2.0 ± 0.1
^{58}Ni	5.9 ± 0.6	1.6 ± 0.3
^{60}Ni	7.7 ± 0.5	1.9 ± 0.3
^{62}Ni	8.6 ± 0.4	1.7 ± 0.4
^{64}Ni	8.4 ± 0.1	0.6 ± 0.1
^{64}Zn	5.9 ± 0.4	2.3 ± 0.9
^{66}Zn	6.9 ± 0.2	1.3 ± 0.5
^{70}Ge	6.9 ± 0.2	2.1 ± 0.4

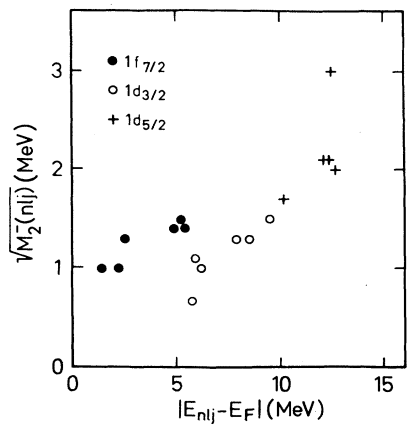

FIG. 7. Widths of the proton hole strength distributions vs energy distance $|E_{nlj} - E_F|$ to the Fermi surface for nickel and zinc isotopes.

consistent analyses have been performed. In Fig. 7 we have plotted the widths $\sqrt{M_2^-(nlj)}$ from Table IV for proton holes in the "inner" $1f_{7/2}, 1d_{3/2}$, and $1d_{5/2}$ shells of nickel and zinc isotopes versus the distance of the respective single-particle energies E_{nlj} to the Fermi energy E_F. As for these shells no stripping strengths have been found, M_2^- represents the total spreading width M_2.

Figure 7 shows that the widths increase with increasing distance to the Fermi surface. At a distance from the Fermi energy of about 5.5 MeV, the widths of $1f_{7/2}$ proton hole states appear to be larger than those of $1d_{3/2}$ hole states. This indicates that the spreading depends on the shell structure. In a more global picture, a quadratic increase $\Gamma^{\downarrow} \sim |E_{nlj} - E_F|^2$ of the spreading widths with increasing distance to the Fermi surface has been proposed by Bertsch *et al.* [32] on the basis of calculations on infinite Fermi liquids. The data of Fig. 7 indicate a different dependence: the observed $1f_{7/2}$ widths close to the Fermi energy are incompatible with the quadratic energy dependence. Also we do not observe a linear energy dependence as predicted to arise from the coupling of surface excitations to single-particle motion of a Fermi liquid [33]. For the investigated nuclei nonvanishing widths are observed even very close to the Fermi energy in contrast to the theoretical predictions which, of course, ignore the details of nuclear structure such as fragmentation due to configuration mixing or deformation. In addition, we see shell-dependent features of the widths, which are also not predicted.

V. SUMMARY

The present ^{66}Zn($\vec{d}$,^{3}He)^{65}Cu experiment led to spin and parity assignments of isolated low-lying ^{65}Cu levels and the localization of inner proton shells in the continuum region. In spite of the limited energy resolution, by the use of a strip-detector telescope, data could be obtained which allowed a reliable decomposition of the spectra with measured angular distributions of differential cross sections and analyzing powers. A DWBA analysis yielded the strength distributions of the different shells from which the lowest-energy moments were calculated. The comparison with results from other proton pickup and stripping reactions on ^{54,56,58}Fe, ^{58,60,62,64}Ni, ^{64}Zn, and ^{70}Ge yielded — after a careful normalization — a compilation of proton single-particle properties. The second moments of the hole strength distributions exhibit mass- and shell-dependent effects not predicted by theories of hole state damping.

This work has been supported in part by the Kernforschungszentrum Karlsruhe.

[1] V. Bechtold, L. Friedrich, P. Doll, K.T. Knöpfle, G. Mairle, and G.J. Wagner, Phys. Lett. **72B**, 169 (1977).
[2] A. Stuirbrink, G.J. Wagner, K.T. Knöpfle, Liu Ken Pao, G. Mairle, H. Riedesel, K. Schindler, V. Bechtold, and L. Friedrich, Z. Phys. A **297**, 307 (1980).
[3] G. Mairle, G.J. Wagner, K.T. Knöpfle, Liu Ken Pao, H. Riedesel, V. Bechtold, and L. Friedrich, Nucl. Phys. **A363**, 413 (1981).
[4] P. Grabmayr, G. Mairle, U. Schmidt-Rohr, G.P.A. Berg, J. Meissburger, P. von Rossen, and J.L. Tain, Nucl. Phys. **A469**, 285 (1987).
[5] N.J. Ward and J.K. Tuli, Nucl. Data Sheets **47**, 135 (1986).
[6] B. Zeidman and J.A. Nolen, Phys. Rev. C **18**, 2122 (1978).
[7] D. Bachner, R. Bock, H.H. Duhm, R. Santo, R. Stock, and S. Hinds, Nucl. Phys. **A99**, 487 (1967).
[8] J.A. Cameron, V.P. Janzen, R.B. Schubank, and E.E. Habib, Nucl. Phys. **A425**, 433 (1984).
[9] M. Seeger, Th. Kihm, K.T. Knöpfle, G. Mairle, U. Schmidt-Rohr, J. Hebenstreit, J. Paul, and P. von Rossen, Nucl. Phys. **A533**, 1 (1991).
[10] M. Seeger, Th. Kihm, K.T. Knöpfle, G. Mairle, and U. Schmidt-Rohr, Nucl. Phys. **A539**, 223 (1992).
[11] G. Mairle, M. Seeger, M. Ermer, P. Grabmayr, A. Mondry, and G.J. Wagner, Nucl. Phys. **A543**, 558 (1992).
[12] R.G. Couch, J.A. Biggerstaff, F.G. Perey, S. Raman, and K.K. Seth, Phys. Rev. C **2**, 149 (1970).
[13] N.G. Puttaswamy, W. Oelert, A. Djaloeis, C. Mayer-Böricke, P. Turek, P.W.M. Glaudemans, C.B. Metsch, K. Heyde, M. Waroquier, P. van Isacker, G. Wenes, V. Lopac, and V. Paar, Nucl. Phys. **A401**, 269 (1983).
[14] K. Reiner, P. Grabmayr, G.J. Wagner, S.M. Banks, B.G. Lay, V.C. Officer, G.G. Shute, B.M. Spicer, C.G. Glover, W.P. Jones, D.W. Miller, H. Nann, and E.J. Stephenson, Nucl. Phys. **A472**, 1 (1987).
[15] A. Marinov, W. Oelert, S. Gopal, G.P.A. Berg, J. Bojowald, W. Hürlimann, I. Katayama, S.A. Martin, C. Mayer-Böricke, J. Meissburger, J.G.M. Römer, M. Rogge, J.L. Tain, P. Turek, P. Zemło, R.B.M. Mooy, P.W.M. Glaudemans, S. Brant, V. Paar, M. Vouk, and V. Lopac, Nucl. Phys. **A431**, 317 (1984).
[16] G. Rau, P. Grabmayr, P. Woldt, V. Pugatch, and G.J.

Wagner, J. Phys. G **18**, 525 (1992).
[17] D.D. Armstrong and A.G. Blair, Phys. Rev. **140**, B1226 (1965).
[18] B. Rosner and C.H. Holbrow, Phys. Rev. **154**, 1080 (1967).
[19] A.G. Blair and D.D. Armstrong, Phys. Rev. **140**, B1567 (1965).
[20] R.M. Britton and D.L. Watson, Nucl. Phys. **A272**, 91 (1976).
[21] R.R. Betts, S. Mordechai, D.J. Pullen, B. Rosner, and W. Scholz, Nucl. Phys. **A230**, 235 (1974).
[22] A. Pfeiffer, G. Mairle, K.T. Knöpfle, Th. Kihm, G. Seegert, P. Grabmayr, G.J. Wagner, V. Bechtold, and L. Friedrich, Nucl. Phys. **A455**, 381 (1986).
[23] S. Khan, G. Mairle, K.T. Knöpfle, Th. Kihm, Liu Ken Pao, P. Grabmayr, G.J. Wagner, and L. Friedrich, Nucl. Phys. **A481**, 253 (1988).
[24] Th. Kihm, G. Mairle, P. Grabmayr, K.T. Knöpfle, G.J. Wagner, V. Bechtold, and L. Friedrich, Z. Phys. A **318**, 205 (1984).
[25] M. Brendle, M. Ermer, P. Grabmayr, and A. Mondry, Nucl. Instrum. Methods **A302**, 342 (1991).
[26] G. Mairle, K.T. Knöpfle, H. Riedesel, G.J. Wagner, V. Bechtold, and L. Friedrich, Nucl. Phys. **A339**, 61 (1980).
[27] R.W. Barnard and G.D. Jones, Nucl. Phys. **A108**, 641 (1968).
[28] S. Khan, Th. Kihm, K.T. Knöpfle, G. Mairle, V. Bechtold, and L. Friedrich, Phys. Lett. **156B**, 155 (1985).
[29] J.H. Bjerregaard, O. Nathan, S. Hinds, and R. Middleton, Nucl. Phys. **85**, 593 (1966).
[30] G. Mairle, Z. Phys. A **322**, 173 (1985).
[31] R.K. Bansal and J.B. French, Phys. Lett. **11**, 14 (1964); **19**, 223 (1965).
[32] G. Bertsch, P.F. Bortignon, and R.A. Broglia, Rev. Mod. Phys. **55**, 287 (1983).
[33] H. Esbensen and G. Bertsch, Phys. Rev. Lett. **52**, 2257 (1984).